1991ApJ...373..110C

THE ASTROPHYSICAL JOURNAL, 373:110–122, 1991 May 20

THE GAS-PHASE CHEMISTRY OF ORGANIC MOLECULES IN INTERSTELLAR CLOUDS WITH DYNAMICAL MIXING

J.-P. CHIÈZE,[1] G. PINEAU DES FORÊTS,[2] AND ERIC HERBST[1,3]

Received 1990 August 22; accepted 1990 November 5

ABSTRACT

In simple pseudo–time-dependent models of the gas-phase chemistry of dense interstellar clouds in which there is more elemental oxygen than carbon, the calculated abundances of organic molecules peak at a so-called "early time" of 1–3 × 10^5 yr before decreasing markedly to steady state values. The large observed abundances of these molecules in dark clouds such as TMC-1 as well as in extended regions of the cores of giant clouds are accounted for in pseudo–time-dependent models only at or near "early time." Since the actual ages of dense interstellar clouds are much larger than 10^5 yr, it is desirable that a mechanism be elucidated which preserves the calculated early-time abundances for much longer periods of time. One such mechanism stems from the phenomenon of dynamical mixing of gaseous material between diffuse regions and denser portions of interstellar clouds. As originally discussed by Chièze and Pineau des Forêts, such dynamical mixing can continually transfer large amounts of neutral and singly ionized atomic carbon into the dense cloud gas; these species, normally present in large abundance only at or before "early time" in simple one-phase models, enhance the synthesis of organic molecules. The possibility thus exists that mixing can lead to large calculated abundances of organic molecules in dense gas at times much later than 10^5 yr and even obliterate the distinction between early time and steady state. In this paper, we present model calculations which show the situation to be somewhat more complex than this. If one considers mixing between diffuse and dense clumps with no gas intermediate in density, it is necessary to mix in large amounts of neutral atomic carbon rather than the singly ionized variety to maintain high abundances of organic molecules at $t \gg 10^5$ yr. If, on the other hand, one considers a more natural model in which gas condensation occurs before mixing, the very act of compression is a significant source of complex molecules. Furthermore, high abundances of organic molecules are preserved for a large range of mixing times.

Subject headings: interstellar: abundances — interstellar: molecules — molecular processes

1. INTRODUCTION

The gas phase chemistry of dense interstellar clouds has been studied by many scientists since the pioneering work of Herbst & Klemperer (1973). For a recent review, see Herbst & Millar (1991). Herbst & Klemperer (1973) utilized a steady state model to calculate molecular abundances and found reasonable agreement between theory and observation for a variety of small molecules. Prasad & Huntress (1980a, b) extended the size of the model greatly and solved the time-dependent chemical kinetic equations while holding the physical conditions (temperature, gas density) constant. This approach is now referred to as the "pseudo–time-dependent" method. Although Prasad & Huntress (1980a, b) discussed some aspects of time-dependent chemistry, their main focus of attention was still on the steady state results, which are achieved in 10^7 yr or more. In general, their steady state results are also in good agreement with observation for a significant number of species. This agreement was and is somewhat puzzling because of the short time scale for adsorption of gas phase species onto the surfaces of dust particles ($t \approx 3 \times 10^9/n$ in yr, where n, the gas density, is given in cm^{-3}; see Winnewisser & Herbst 1987) and the apparent absence of efficient desorption mechanisms. Still, the existence of good agreement between theory and observation was a powerful inducement to ignore this problem.

The realization that simple one-phase steady state gas phase chemistry could not explain all of the observational data with the exception of H_2 began with the observation of large abundances of neutral atomic carbon by Phillips and co-workers (Phillips & Huggins 1981; Keene et al. 1985) since such large abundances, if coming from dense gas within clouds, are incompatible with standard oxygen-rich models, in which most carbon is tied up in the form of carbon monoxide. As shown by Langer and co-workers (Graedel, Langer, & Frerking 1982; Langer et al. 1984; Langer & Graedel 1989) who were the first to focus on the time-dependent aspects of the carbon chemistry, large amounts of neutral atomic carbon exist at times well before steady state is achieved, so that one explanation for the observations is that the chemistry has not yet reached steady state conditions. Another school of thought was that the atomic carbon arises from outer regions of dense clouds subjected to strong ultraviolet radiation fields which can photodissociate carbon monoxide, such as exist on the borders with H II regions (Tielens & Hollenbach 1985a, b). This latter explanation has undergone modification due to the clumpy nature of clouds (see below). In either case, something more complex than a steady state one-phase chemical model is required to explain the neutral atomic carbon abundances unless the material is carbon-rich or below standard densities (Langer et al. 1984; Langer & Graedel 1989). The possibility that cosmic-ray–induced ultraviolet radiation, which exists deep inside dense cloud cores and which does result in some

---

[1] Commissariat à l'Energie Atomique, Centre d'études de Bruyères-le-Châtel, Service PTN, F-91680 Bruyères-le-Châtel, France.

[2] DAMAp, Observatoire de Paris, F-92195 Meudon Principal Cedex, France.

[3] Permanent address: Department of Physics, Duke University, Durham, NC 27706.

photodissociation of carbon monoxide, can produce enough C to explain the observations has also been considered (Prasad & Tarafdar 1983; Gredel, Lepp, & Dalgarno 1987; Langer & Graedel 1989).

Steady state gas phase chemistry also apparently fails to explain the observed abundances of organic molecules. Species such as the cyanopolyynes or complex oxygenated molecules can be observed with fractional abundances in the range 10^{-8}–10^{-10}. A collection of the observed fractional abundances in the well-studied source TMC-1 is contained in Herbst & Leung (1989; hereinafter HL) and is discussed in the next section. Leung, Herbst, & Huebner (1984) and Millar & Nejad (1985) were the first to include the gas phase chemistry of a variety of moderately complex molecules in pseudo–time-dependent treatments. They showed that calculated abundances of organic molecules are, unlike those of smaller species, strongly time dependent, increasing up to a time of 1–3 × 10^5 yr before decreasing strongly to steady state values. However, their qualitative results were quite different from one another; Leung et al. achieved good agreement with observations with their peak abundances whereas Millar & Nejad (1985) achieved reasonable agreement at steady state. These initial discrepancies were soon rationalized by Millar, Leung, & Herbst (1987) in terms of a small number of unstudied chemical reactions involving atomic oxygen. If these destructive reactions occur rapidly, and the dominant school of thought is that this is indeed the case, then pseudo–time-dependent gas phase models lead to the prediction that abundances of organic molecules in agreement with observation exist only 1–3 × 10^5 yr after the chemistry onsets, a time interval now referred to as "early time." The large abundances of organic molecules derive from the chemical precursors C and C^+ via the initial reactions

$$C + H_3^+ \rightarrow CH^+ + H_2 , \quad (1)$$

$$C^+ + H_2 \rightarrow CH_2^+ + h\nu , \quad (2)$$

which have been studied extensively via theoretical means (Smith 1989; Talbi & De Frees 1990) and by subsequent reactions involving C and C^+ (Winnewisser & Herbst 1987). As mentioned above, in oxygen-rich one-phase models which ignore ultraviolet radiation, these precursors are abundant only at times well before steady state is achieved. The inclusion of cosmic-ray–induced ultraviolet radiation does not change the calculated molecular abundances dramatically (Gredel et al. 1989).

HL and Herbst & Leung (1990) have now extended the one-phase, pseudo–time-dependent approach to include 2577 gas phase chemical reactions involving 276 species of up to nine carbon atoms in size. Their results show that the abundances of both small and large molecules in the well-studied source TMC-1 are in the main well accounted for at early time, although there are several important exceptions. Millar & Herbst (1990) have produced similar models to study the chemistry of sulfur-bearing molecules and prefer a time slightly longer than "early time" for best agreement with observation. Brown & Charnley (1990) have shown that inclusion of adsorption onto dust particles does not vitiate the early-time agreement with observation for at least the smaller molecules presently included in their model, but actually (and counterintuitively) pushes back the time for optimum agreement. Even more recently, Flower & Pineau des Forêts (1990) have reported that a more detailed consideration of the thermal evolution of dense clouds including the formation of H_2 on grains shows that large amounts of C (and even C^+) can be maintained for periods of more than 10^6 yr, which might lead to a similar maintenance of large abundances of organic molecules. Such large abundances can be postponed to longer time scales in models with gravitational collapse because at low initial densities the chemistry is rather slow (Tarafdar et al. 1985). Our calculations show that if the initial form of atomic carbon is neutral rather than ionized, the early-time abundances are achieved at virtually the same time as in standard calculations, which start with H_2 and C^+. Thus it would appear that one-phase chemical models of varying complexity can reproduce most if not all of the observed molecular abundances in non–star-forming regions of dense cloud cores in times between 10^5 and 10^6 yr after the onset of chemistry. The peak early-time abundances themselves are surprisingly insensitive to a wide range of initial chosen abundances.

Although the agreement between dense cloud observations and one-phase chemical models at times before steady state is achieved is gratifying, it is well known that interstellar clouds are not simple regions at constant density. On the contrary, density variations are observed and/or inferred over a wide range of length scales from large cores to small star-forming regions (Scalo 1990). The denser portions of material are often referred to as clumps although the topology of the material may be quite complex. The contrast between the denser and more diffuse regions may also be highly variable. Perhaps the strongest contrast exists in clouds near strong sources of ultraviolet radiation where photodissociation regions are inferred since the large amounts of C and C^+ detected in such regions imply a very diffuse interclump medium (Genzel et al. 1988; Stutzki et al. 1988). On the other hand, dark clouds such as TMC-1 are themselves condensations of size ≈ 1 pc formed from only a somewhat more diffuse gas. In any event, the existence of a diffuse medium surrounding dense clumps of gas can strongly affect the gas phase chemistry of the dense material if, as originally suggested by Chièze & Pineau des Forêts (1989 hereafter CPF1), mixing of material occurs between the two phases. The chemistry of the dense material can also be influenced by newly formed stars, as has been investigated by Williams and co-workers (Williams 1988; Charnley et al. 1988a, b).

Two approaches to the problem of cloud clumping have recently been formulated. In one (Chièze & Pineau des Forêts 1989), the mass distribution of material in clouds as a function of density is posited to derive from stretched gravitational collapse and relaxation. In a second approach (de Boisanger & Chièze 1990; Chièze & Pineau des Forêts 1990 hereafter CPF2), local variations of the ultraviolet radiation field intensity trigger the formation and destruction of dense regions in a more diffuse medium. In addition, collective motions are induced which can lead to chemical mixing. These motions are currently being studied via a two-dimensional hydrodynamic code by de Boisanger & Chièze (private communication).

CPF1 and CPF2 have considered a chemical mixing model in which two or three parcels of gas at differing but generally fixed physical conditions coexist. In each of these parcels, the gas phase chemistry can be followed. A small chemical network connecting 50 atomic and small molecular species was utilized. In the two-phase model, one parcel of gas represents dense material whereas the second represents diffuse material. In the three-phase model, a parcel with characteristics in between diffuse and dense material was also included. Among these

1991ApJ...373..110C

parcels mixing of material occurs with characteristic mixing times according to equations in which the amount and direction of mixing depends upon abundance gradients. In their two-phase model, CPF1 and CPF2 followed the chemistry of the dense clump or parcel in the limit in which the diffuse interclump material is much more massive so that the mixing only affects the dense material to a first approximation. Among the interesting chemical effects they found was that short mixing times (<1 Myr) greatly enhance the abundances of C and C^+ in the dense material at steady state. An enhancement in C and C^+ might be expected to lead to an enhancement in organic molecules with syntheses starting from reactions (1) and (2) (HL). Indeed, such an enhancement was found for the few polyatomic molecules in the model such as C_3H_2, raising the possibility that the strong time dependence of organic molecule abundances in simple one-phase models could in general be diminished or even eliminated in the dense portions of two or more phase models with rapid mixing. In addition, the choice of initial abundances would certainly be unimportant if steady state solutions could be utilized. However, the original chemical model used by CPF1 and CPF2 did not contain sufficient complex molecules to allow a determination of the detailed effect of dynamical mixing as regards organic species.

It is therefore the purpose of this paper to explore in detail the suggestion raised by CPF1 that rapid mixing can indeed preserve large abundances of organic molecules well past the so-called early time of pseudo–time-dependent models. To determine the validity of the suggestion, the large chemical network of HL has been utilized in two types of models with dynamical mixing. The first type is a simple two-phase model with variable mixing rates. Our results from this type of model show that mixing of diffuse cloud gas into dense material does indeed tend to increase the steady state abundances of organic molecules. However the enhancements at steady state are not in general sufficiently large to reproduce the early-time abundances of one-phase models *unless the diffuse material is rich in neutral atomic carbon rather than singly ionized carbon.* The second type of model is a more realistic one, in which it is recognized that dynamical mixing between diffuse and dense gas occurs through gas of continually varying density rather than through a discontinuous step. In this model, large complex molecule abundances are achieved at steady state in a more natural manner.

The remainder of the paper is divided as follows. In § 2, the chemical and dynamical aspects of the simple two-phase model are reviewed and the results are discussed. Our more realistic model is considered in § 3, along with representative results. Finally, our conclusions are stated in § 4.

2. SIMPLE TWO-PHASE MODEL

2.1. *Chemistry and Dynamics*

The chemistry of two parcels of material has been followed simultaneously. These parcels are defined by the following fixed parameters: their total masses, their gas densities, expressed rigorously in terms of mass or approximately in terms of $n_{\mathrm{H}} = n(\mathrm{H}) + 2n(\mathrm{H}_2)$, the radiation field incident upon them, and their visual extinctions. The temperatures of the parcels are followed by suitable heating and cooling rates (Chièze & Pineau des Forêts 1987). The thermal equilibrium of the dense parcel is dominated by heat exchange between the gas and the dust (Black 1987). We have adopted here a grain temperature of 15 K. In the diffuse region, the gas temperature results essentially from the balance between heating via the photoelectric effect on dust grains (Boland & de Jong 1984) and C^+ cooling (Flower, Pineau des Forêts, & Hartquist 1986). It varies from 115 to 53 K depending on the C^+ abundance. However, we have checked that the calculated abundances depend only weakly on the gas temperatures.

TABLE 1

PHYSICAL PARAMETERS OF GAS PARCELS

Parameter	Parcel 1	Parcel 2
$n_{\mathrm{H}}\,(\mathrm{cm}^{-3})$	2.0×10^4	100.
T (K)	17	53–115[a]
A_V	10.0	0.5

[a] Representative numbers only. Actual temperatures are calculated according to the discussion in the Appendix and depend on the C^+ abundance.

Table 1 summarizes the physical conditions that define the parcels of gas in our two-phase models. The model can be thought of as representing either a diffuse cloud envelope and dense core or a diffuse medium surrounding dense clumps. The denser parcel has the physical characteristics of dark clouds such as TMC-1. The chemical network used for both parcels is that of HL with slow reaction rates and low metal abundances. The expected agreement between our results in the absence of mixing with their results has been confirmed at both early time and steady state. As mentioned above, we have, however, started with carbon in the form of C rather than the customary C^+. As previously, it is assumed that molecular hydrogen is self-shielded in all parcels.

In addition to the changes in the concentrations of species caused by chemistry, mixing among the parcels is included via the equations

$$dn_x^{(i)}/dt = N_x^{(i)} - (n_x^{(i)} - (\rho^{(i)}/\rho^{(j)})n_x^{(j)})t^{(i)}_{\mathrm{mix}-1}\ , \tag{3}$$

where $n_x^{(i)}$ is the concentration of species x in parcel (i), $N_x^{(i)}$ is its rate of change due to chemical reactions, $\rho^{(i)}$ and $\rho^{(j)}$ are the densities of parcels (i) and (j), and $t^{(i)}_{\mathrm{mix}}$ is the mixing time for parcel (i), which is itself given by the equation

$$t^{(i)}_{\mathrm{mix}} = M^{(i)}/dM/dt\ , \tag{4}$$

where $M^{(i)}$ is the overall mass of the parcel and dM/dt is the constant mass exchange rate between the two parcels, whose masses are conserved. Equations (3)–(4) are derived in the Appendix as is the time dependence of the temperature. The network of chemical-mixing equations used in this work has been solved via a standard Gear algorithm. In the studies described below, the masses of the diffuse parcels of gas are assumed to be much larger than those for the dense parcels and, consequently, the mixing times for diffuse parcels of gas are set at large values so that only the dense parcels, representing small portions of the cloud, are affected significantly by mixing. Note that mixing modifies the abundance of a given chemical species until the ratio of its number densities in the two parcels being mixed equals the ratio of the total mass densities in the parcels.

2.2. *Results*

Figures 1–3 illustrate some typical results of the two-phase mixing models as they relate to the dense parcel of gas.

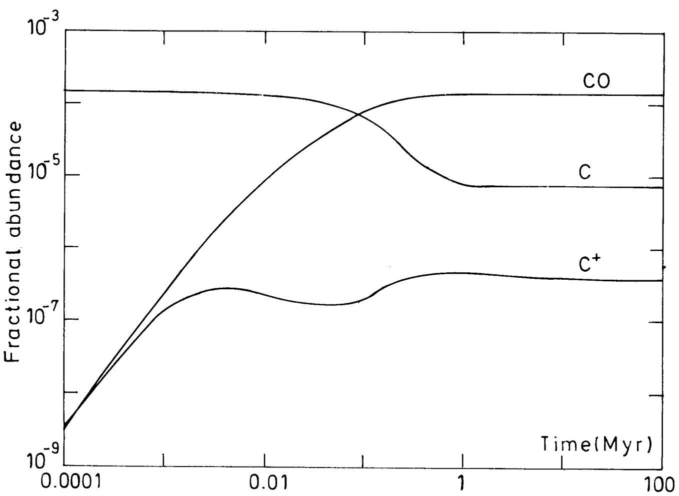

FIG. 1.—The fractional abundances of C^+, C, and CO with respect to H_2 in the dense parcel of gas of the two-phase model are plotted vs. time. Mixing time $t_{\rm mix}^{(1)} = 0.5$ Myr.

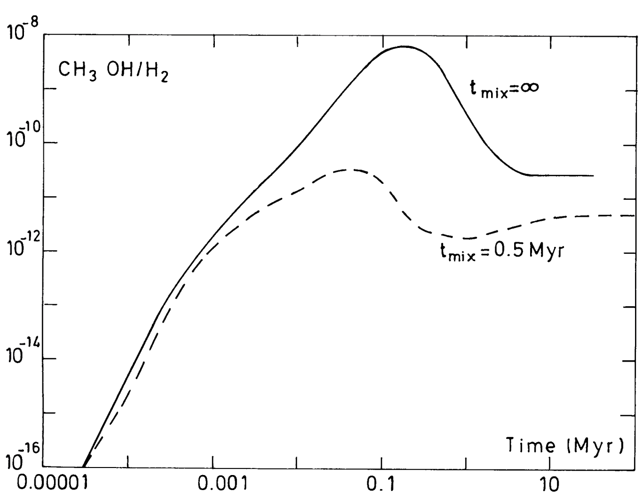

FIG. 3.—The fractional abundance of CH_3OH with respect to H_2 is plotted vs. time for a model without mixing (*solid line*) and for the dense parcel of gas in a two-phase model in which the mixing time is 0.5 Myr. (*dashed line*).

Although results with mixing times $t_{\rm mix}^{(1)}$, where (1) refers to the dense parcel, from 2 Myr down to 0.1 Myr have been considered, a representative mixing time of 0.5 Myr is used for the figures. In these figures selected fractional abundances with respect to $n(H_2) = 1.0 \times 10^4$ cm^{-3} are plotted versus time in Myr. Figure 1 shows the three important species C^+, C, and CO. The time dependence of C^+ is most different from one-phase models; given our choice of C as the initial repository of elemental carbon, one might expect the abundance of C^+ to increase initially from its initial value of "zero" and then to decrease. Indeed, as the chemistry commences, C^+ increases in abundance and then begins to decrease, as expected. However, unlike one-phase models, the C^+ abundance then begins to increase anew until reaching its steady state value in ≈ 1 Myr. By this time, C^+ has become the dominant ion with a fractional abundance of 3.8×10^{-7} and the overall fractional ionization is consequently much larger than in one-phase models with depleted metal abundances, where it is typically less than 10^{-7} (HL). The large abundance of C^+ stems from the injection of diffuse gas rich in this species. The choice of physical conditions of the diffuse parcel of gas ($n_{\rm H} = 10^2$ cm^{-3}, $A_V = 0.5$) guarantees that it will be rich in ionized atomic carbon after a short period of time. The time dependence of the fractional C abundance in Figure 1 is essentially monotonically downward but at steady state the abundance is still orders of magnitude larger than in standard one-phase models of dense gas. The additional C derives from mixing and chemical processing of C^+. The CO abundance in Figure 1 is little affected by the process of mixing.

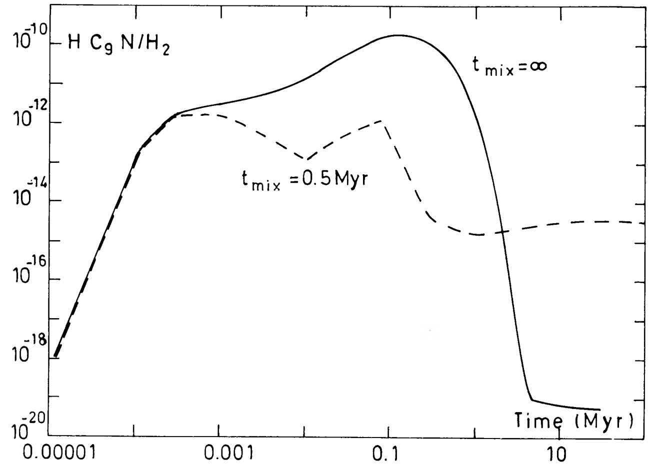

FIG. 2.—The fractional abundance of HC_9N with respect to H_2 is plotted vs. time for a model without mixing (*solid line*) and for the dense parcel of gas in a two-phase model in which the mixing time is 0.5 Myr. (*dashed line*).

Since there are both large amounts of C and C^+ in the dense gas at steady state, one might expect enhanced abundances of organic molecules. However, one must be cautious because the high fractional ionization will tend to reduce complex molecule abundances somewhat (HL). A major reason for this destructiveness is simply ion-molecule reactions between the neutrals and C^+. In addition to this effect, there is also the previously recognized effect (HL) that high electron abundances preferably deplete molecular ions important as intermediates in synthesis. Moreover, although it is not dominant at the mixing time chosen, there is the extra loss term due to material flowing out of the dense parcel.

In Figures 2–3, the fractional abundances of two representative organic molecules—HC_9N and CH_3OH—are plotted versus time for our mixing model and for a model in which no mixing is allowed. The plot of HC_9N versus time (Fig. 2) represents the normal pattern in which, despite inducing a rather complex pattern, mixing tends to obliterate the large difference between early-time and steady state abundances of nonmixing models by reducing the early-time abundances and increasing the steady state abundances. The increase at steady state presumably occurs because the synthetic power of the additional C and C^+ outweighs the destructiveness of high fractional ionization. The decrease at early time stems mainly from the high ionization since there is a large amount of C at early time in both mixing and nonmixing models. In Figure 3, it can be seen that the case of methanol is somewhat different in that mixing at the rate chosen does not result in an increased steady state abundance. Presumably, the high ionization and (secondarily) the loss due to mixing are more important than the increased synthetic power of C and C^+ in this case.

Although these results show that mixing between diffuse and dense parcels of gas does tend to obliterate the large differences between early-time and steady state abundances, the results cannot be said to be totally satisfactory in that the peak early-time organic molecule abundances, needed by and large to explain observations in TMC-1 and other sources (HL), are reduced. In other words, although we have succeeded in reducing the extreme and possibly artifical time dependence of the organic molecule abundances in one-phase pseudo–time-dependent models, we have not succeeded in maintaining these abundances at the large early-time values of one-phase models. In order to determine whether our results can be improved by varying the mixing time $t_{\rm mix}^{(1)}$, we have varied this parameter widely. Table 2 contains selected fractional abundances of molecules in the dense parcel of gas at steady state for mixing times ranging from 2 Myr down to 0.1 Myr. Our steady state and peak early-time abundances in the limit of no mixing are also included as is a list of observed abundances in TMC-1. The observed abundances of complex molecules far exceed the calculated steady state abundances in the limit of no mixing and are in much better agreement with the early-time abundances, although these peak abundances can be too large for selected species, especially with the nonrapid ion-polar reaction rates utilized here. A detailed discussion of the agreement between calculated early-time abundances in the limit of no mixing with observation in TMC-1 is contained in HL.

It can be seen in Table 2 that although more rapid mixing rates increase the abundances of *some* organic molecules in the model and smaller but nonzero mixing rates increase the abundance of others, the enhanced abundances are typically much lower than the peak early-time abundances in the limit of no mixing, especially for the more complex organic species. The organic molecules with abundances that are decreased at very high mixing rates are no doubt especially sensitive to the overall ionization fraction. We conclude that our simple two-phase model cannot reproduce at steady state the large organic molecule abundances obtained at early time in the limit of no mixing.

Large mixing rates also wreak havoc on some of the calculated small molecule abundances. For example, the calculated ammonia fractional abundance of 6.4×10^{-12} at the highest mixing rate shown in Table 2 is over three orders of magnitude below its observed value ($\approx 10^{-8}$) in both dark clouds and extended portions of giant clouds such as the extended ridge in Orion. In addition, the calculated abundance of HNC drops precipitously. The problem appears once again to be the high degree of ionization caused by the large C^+ abundance. Indeed, a high degree of ionization leads to poor agreement with observation for many small molecules, a fact noted by Graedel et al. (1982).

2.3. *Importance of Neutral Atomic Carbon*

Given the problem, it appears natural to attempt a different model in which the diffuse gas is rich in neutral C rather than C^+. This cannot be done naturally in our simple two-phase model because, as shown by van Dishoeck & Black (1988), the dominant form of carbon in diffuse gas tends to be either C^+ or CO depending on the depth (or A_V) into the cloud. A CO-rich diffuse gas does not enhance organic model abundances via mixing. Variation of both the density and visual extinction of the diffuse parcel shows only a small improvement in the steady state organic molecule abundances, mainly because of the difficulty in obtaining diffuse gas in which C dominates. It is possible, however, to obtain models in which the early-time abundances approach those of the one-phase models. One method of obtaining a gas rich in C is to consider in some detail what happens to C^+ as it mixes into the dense region. This is undertaken in § 3. In the context of the simple two-phase model, however, we are forced to increase the C/C^+ abundance ratio in the diffuse parcel artificially, as discussed below.

Table 3 contains selected steady state results ($t > 10^7$ yr) for fractional molecular abundances in the dense parcel of gas with a mixing time $t_{\rm mix}^{(1)} = 0.2$ Myr as functions of the C/C^+ abundance ratio in the diffuse parcel. The results are shown for five models, which are defined in the following manner: model 5 is our standard two-phase calculation whereas models 1–4 are altered by lowering the carbon photoionization rate, thereby raising the C/C^+ abundance ratio in the diffuse parcel of gas. The carbon photoionization rate is multiplied by factors of 0, 1.7×10^{-4}, 7.5×10^{-4}, and 3.4×10^{-3}, respectively in models 1–4. The resulting C/C^+ abundance ratios in the diffuse parcels of gas are shown at the top of Table 3. It can be seen that this ratio is largest in model 1 and decreases as the model number increases, with the minimum value of 2.6×10^{-3} in model 5, our realistic diffuse cloud. In addition to the steady state results of models 1–5, we have also listed for comparison the early-time results of HL for depleted metal abundances and slow reaction rates. (The good agreement between the early time results of these authors and of ourselves can be compared by glancing at Tables 2 and 3; the slight differences are caused by the somewhat different times chosen and by differences in A_V).

For all models 1–5 in Table 3, there is a large amount of neutral atomic carbon in the dense gas, distinguishing it from one-phase steady state models. As the model number decreases from 5 to 1, the C^+ abundance and fractional ionization in the dense parcel decrease strongly. Indeed, in model 1, the large C abundance coupled with the low fractional ionization of 4.5×10^{-8} make this model resemble the conditions normally associated with early time in one-phase models. *Not surprisingly, therefore, the calculated steady state abundances for model 1 are in excellent agreement with the early-time abundances of one-phase models, especially for the most complex molecules in the network. With increasing model number and thus increasing fractional ionization, the calculated molecular abundances depart from the early-time abundances.* It is interesting to observe that the largest abundance differences among models 1–5 often involve the most complex organic species. Since the one-phase early-time results are in good agreement with observation for the well-studied dark cloud TMC-1 (especially if rapid ion-polar rates are utilized), our mixing model can represent this cloud well at steady state if the gas mixing into the dense parcel is exceedingly rich in C and poor in C^+. Because the one-phase early-time results can be too large for selected large molecules, even in TMC-1, it might be possible to fine tune the agreement between observation and our two-phase steady state models by decreasing the C/C^+ ratio in the diffuse parcel from its value in model 1. But a diffuse gas with a significant abundance of C^+ would not really resemble the material surrounding TMC-1 or other dark clouds. Our steady state models with high C^+ in the diffuse gas may well represent other sources with smaller abundances of complex organic species, especially if the dense parcels of gas are imbedded in very diffuse gas. M17 represents an interesting test case.

TABLE 2

SELECTED CALCULATED FRACTIONAL ABUNDANCES[a] AT STEADY STATE FOR THE DENSE PORTION OF THE TWO-PHASE MODEL VERSUS $t^{(1)}_{\rm mix}$ (Myr)

	One-Phase Models		TMC-1	Two-Phase Models			
				$t^{(1)}_{\rm mix}$			
Species	Early-time (0.22 Myr)	Steady-state		2.0	1.0	0.5	0.1
e	3.4(-08)	3.5(-08)		6.6(-08)	2.0(-07)	5.8(-07)	2.4(-06)
C^+	3.1(-09)	1.2(-09)		2.0(-08)	1.0(-07)	3.8(-07)	2.0(-06)
OH	1.3(-07)	5.7(-07)	3(-07)	1.3(-07)	1.4(-07)	8.1(-08)	4.3(-08)
CH	1.5(-08)	3.6-10)	2(-08)	2.0(-09)	1.2(-08)	4.9(-08)	2.6(-07)
NH	3.5(-10)	1.2(-08)		2.2(-09)	1.4(-09)	2.2(-10)	4.6(-11)
CO	1.1(-04)	1.5(-04)	8(-05)	1.5(-04)	1.4(-04)	1.4(-04)	1.1(-04)
C_2	1.0(-08)	1.0(-10)	5(-08)	1.2(-09)	6.8(-09)	2.8(-08)	1.8(-07)
CN	8.8(-08)	2.5(-09)	3(-08)	3.8(-09)	1.8(-08)	5.8(-08)	2.4(-07)
NO	7.2(-08)	3.1(-07)		1.6(-07)	1.2(-07)	3.8(-08)	6.5(-09)
CH_2	1.5(-07)	5.2(-10)		5.0(-09)	2.2(-08)	7.0(-08)	2.2(-07)
NH_2	4.4(-09)	1.0(-07)		1.9(-08)	9.5(-09)	9.2(-10)	8.1(-11)
H_2O	8.8(-06)	3.5(-06)		2.4(-06)	7.6(-07)	1.6(-07)	3.3(-08)
C_2H	1.9(-08)	3.7(-10)	8(-08)	1.7(-09)	8.9(-09)	3.3(-08)	1.4(-07)
HCN	8.4(-07)	4.8(-09)	2(-08)	1.0(-08)	1.2(-08)	1.3(-08)	8.1(-09)
HNC	4.5(-07)	5.1(-09)	2(-08)	6.4(-09)	2.4(-09)	4.2(-10)	1.5(-10)
NH_3	1.6(-08)	1.7(-07)	2(-08)	3.5(-08)	5.6(-09)	2.4(-10)	6.4(-12)
C_2H_2	7.5(-07)	5.6(-09)		4.7(-08)	4.6(-08)	4.0(-08)	2.9(-08)
H_2CO	8.3(-07)	9.9(-09)	2(-08)	4.0(-08)	6.4(-08)	6.3(-08)	3.2(-08)
C_3H	4.4(-07)	1.1(-09)	5(-10)	2.0(-08)	2.9(-08)	3.2(-08)	3.8(-08)
C_3N	1.9(-09)	1.4(-12)	1(-09)	6.0(-11)	1.6(-10)	3.0(-10)	4.7(-10)
CH_4	6.1(-06)	1.3(-07)		2.7(-07)	2.5(-07)	2.1(-07)	1.4(-07)
C_3H_2	1.9(-07)	6.2(-10)	2(-08)	1.7(-08)	2.6(-08)	2.9(-08)	3.6(-08)
C_4H	3.5(-07)	1.4(-11)	2(-08)	3.7(-10)	1.1(-09)	3.7(-09)	1.8(-08)
HC_3N	2.5(-08)	3.6(-12)	6(-09)	2.7(-10)	1.9(-10)	9.7(-11)	2.9(-11)
C_5H	6.2(-08)	8.8(-13)	4(-10)	7.5(-11)	6.6(-11)	2.3(-10)	4.5(-09)
CH_3OH	7.8(-09)	2.6(-11)	4(-09)	7.6(-11)	2.5(-11)	4.8(-12)	6.1(-13)
C_6H	1.1(-07)	3.0(-13)	1(-09)	1.5(-10)	1.4(-10)	3.0(-10)	4.7(-09)
HC_5N	1.5(-08)	9.5(-15)	3(-09)	3.8(-12)	5.0(-12)	7.1(-12)	5.8(-12)
C_7H	9.9(-09)	3.1(-15)		2.5(-12)	2.5(-12)	1.6(-12)	4.4(-12)
C_8H	1.8(-08)	7.4(-16)		3.0(-12)	5.4(-12)	1.7(-11)	5.6(-10)
CH_3C_3N	4.6(-10)	2.0(-15)	5(-10)	5.1(-13)	1.5(-13)	3.4(-14)	3.7(-15)
HC_7N	7.8(-10)	2.2(-17)	1(-09)	1.9(-13)	9.8(-14)	8.4(-14)	2.6(-13)
CH_3OCH_3	4.4(-12)	1.1(-16)		1.2(-15)	3.5(-16)	6.0(-17)	4.9(-18)
C_9H	1.3(-09)	1.5(-17)		4.2(-14)	1.9(-14)	1.5(-14)	7.9(-14)
HC_9N	1.6(-10)	5.9(-20)	3(-10)	3.3(-15)	2.8(-15)	3.5(-15)	1.7(-14)
H_3^+	2.5(-09)	3.7(-09)		2.1(-09)	2.9(-09)	2.1(-09)	1.9(-09)
HCO^+	5.7(-09)	1.1(-08)	8(-09)	5.7(-09)	2.7(-09)	7.9(-10)	2.7(-10)
N_2H^+	1.3(-11)	5.7(-10)	5(-10)	1.8(-10)	6.7(-11)	4.8(-12)	5.6(-14)
H_3O^+	3.3(-09)	1.5(-09)		1.3(-09)	6.0(-10)	1.6(-10)	3.9(-11)
CH_3^+	4.7(-11)	4.1(-13)		7.2(-12)	4.0(-11)	1.3(-10)	4.6(-10)

NOTE.—$a(-b)$ refers to a 10^{-b}

[a] With respect to H_2.

TABLE 3

SELECTED CALCULATED FRACTIONAL ABUNDANCES[a] AT STEADY STATE VERSUS C/C^+ IN THE DIFFUSE GAS FOR THE DENSE PARCEL OF THE TWO-PHASE MODEL WITH $t_{\rm mix}^{(1)} = 0.2$ Myr

Species	HL Early-time (0.32 Myr)	Model 1	Model 2	Model 3	Model 4	Model 5 (standard)
$(C/C^+)_{\rm diff}$		300	5.1	1.5	0.49	2.6(-03)
$(C/CO)_{\rm dense}$	0.04	0.81	0.63	0.48	0.32	0.16
$T_{\rm dense}/T_{\rm diffuse}$		17/115	17/108	17/95	17/75	17/53
e	3.4(-08)	4.5(-08)	8.0(-08)	3.0(-07)	7.3(-07)	1.3(-06)
C^+	3.1(-09)	3.6(-09)	2.9(-08)	1.9(-07)	5.4(-07)	1.0(-06)
OH	1.8(-07)	1.1(-07)	9.9(-08)	8.8(-08)	7.8(-08)	7.0(-08)
CH	7.2(-09)	4.6(-08)	4.5(-08)	5.9(-08)	9.0(-08)	1.4(-07)
NH	5.1(-10)	2.0(-10)	1.3(-10)	9.5(-11)	7.8(-11)	6.9(-11)
CO	1.3(-04)	7.4(-05)	8.6(-05)	9.7(-05)	1.1(-04)	1.2(-04)
C_2	6.8(-09)	2.2(-08)	3.3(-08)	4.8(-08)	6.7(-08)	8.7(-08)
CN	6.9(-08)	9.5(-08)	9.8(-08)	1.0(-07)	1.1(-07)	1.4(-07)
NO	1.8(-07)	2.6(-08)	2.7(-08)	2.5(-08)	2.1(-08)	1.7(-08)
CH_2	6.8(-08)	2.8(-07)	2.6(-07)	2.2(-07)	1.8(-07)	1.5(-07)
NH_2	5.4(-09)	3.2(-09)	1.8(-09)	8.2(-10)	3.5(-10)	1.7(-10)
H_2O	8.7(-06)	4.8(-06)	1.9(-06)	4.0(-07)	1.4(-07)	6.5(-08)
C_2H	8.1(-09)	7.2(-08)	6.6(-08)	6.8(-08)	7.4(-08)	8.2(-08)
HCN	5.1(-07)	9.4(-07)	3.8(-07)	7.3(-08)	2.3(-08)	1.1(-08)
HNC	3.4(-07)	3.2(-07)	4.9(-08)	2.0(-09)	4.1(-10)	2.1(-10)
NH_3	1.8(-08)	1.3(-08)	3.5(-09)	4.0(-10)	7.5(-11)	2.3(-11)
C_2H_2	5.4(-07)	5.4(-07)	3.6(-07)	1.2(-07)	5.8(-08)	3.5(-08)
H_2CO	5.5(-07)	6.8(-07)	3.1(-07)	1.3(-07)	7.1(-08)	4.8(-08)
C_3H	3.2(-07)	2.8(-07)	2.2(-07)	9.7(-08)	5.3(-08)	3.6(-08)
C_3N	1.5(-09)	1.7(-09)	1.8(-09)	8.5(-10)	5.1(-10)	4.2(-10)
CH_4	5.3(-06)	3.7(-06)	1.6(-06)	4.8(-07)	2.6(-07)	1.8(-07)
C_3H_2	1.6(-07)	1.2(-07)	1.3(-07)	8.0(-08)	4.7(-08)	3.3(-08)
C_4H	2.0(-07)	2.1(-07)	1.5(-07)	3.4(-08)	1.3(-08)	1.0(-08)
HC_3N	1.6(-08)	1.9(-08)	6.8(-09)	6.5(-10)	1.3(-10)	5.0(-11)
C_5H	3.2(-08)	3.1(-08)	1.1(-08)	1.4(-09)	1.0(-09)	1.4(-09)
CH_3OH	8.4(-09)	4.0(-09)	5.0(-10)	2.6(-11)	4.6(-12)	1.6(-12)
C_6H	5.4(-08)	4.9(-08)	3.0(-08)	3.0(-09)	1.3(-09)	1.4(-09)
HC_5N	7.2(-09)	7.6(-09)	2.4(-09)	1.2(-10)	1.8(-11)	7.1(-12)
C_7H	5.0(-09)	3.6(-09)	1.1(-09)	4.0(-11)	5.0(-12)	2.1(-12)
C_8H	8.3(-09)	6.3(-09)	3.3(-09)	2.0(-10)	9.2(-11)	1.4(-10)
CH_3C_3N	3.0(-10)	2.3(-10)	4.5(-11)	7.4(-13)	4.9(-14)	9.6(-15)
HC_7N	4.1(-10)	3.5(-10)	8.3(-11)	1.9(-12)	2.9(-13)	1.7(-13)
CH_3OCH_3	9.9(-12)	1.7(-12)	5.8(-14)	7.6(-16)	6.8(-17)	1.6(-17)
C_9H	6.1(-10)	3.7(-10)	7.2(-11)	8.3(-13)	7.9(-14)	3.6(-14)
HC_9N	8.0(-11)	5.3(-11)	9.5(-12)	1.1(-13)	1.6(-14)	1.0(-14)
H_3^+	2.5(-09)	1.8(-09)	1.9(-09)	2.0(-09)	2.0(-09)	2.0(-09)

TABLE 3—*Continued*

Species	HL Early-time (0.32 Myr)	Model 1	Model 2	Model 3	Model 4	Model 5 (standard)
HCO^+	5.7(-09)	4.5(-09)	4.3(-09)	1.4(-09)	6.6(-10)	4.1(-10)
N_2H^+	3.2(-11)	7.8(-12)	7.8(-12)	2.7(-12)	9.9(-13)	4.4(-13)
H_3O^+	2.9(-09)	2.4(-09)	1.3(-09)	3.4(-10)	1.3(-10)	7.3(-11)
CH_3^+	1.3(-11)	1.1(-10)	1.1(-10)	1.5(-10)	2.2(-10)	3.0(-10)

NOTE.—*a*(-*b*) refers to a 10^{-b}.
[a] With respect to H_2.

3. THREE-STAGE MODEL

Our most successful two-phase model with mixing in terms of maintaining organic molecule abundances at early time involves a diffuse envelope rich in neutral rather than ionized carbon. The large C/C^+ abundance ratio and large C absolute abundance in the envelope must be obtained artificially since models of diffuse clouds tend to yield either C^+ or CO to be the dominant carbon-containing species. However, the large C abundance derives naturally from a more detailed consideration of the mixing process.

Mixing occurs in reality among parcels of gas with slightly differing physical conditions which all coexist in dense interstellar clouds. As ionized atomic carbon from a diffuse parcel mixes into denser regions of gas, it is converted into C and CO. If the conversion $C^+ \rightarrow C$ occurs substantially in a time shorter than or comparable with the mixing time and if the full conversion into CO requires considerably more time, then the act of dynamical mixing will itself yield the precursor C needed for maintenance of large organic molecule abundances. One calculation in support of this manner of rationalizing the production of precursor C has been undertaken by de Boisanger & Chièze (1990) who followed the chemistry of a contracting clump starting from the initial conditions $n_H = 40$ cm^{-3}, $A_V = 0.25$ using a reduced chemical network. An increase in the visual extinction by 2 triggers the formation of a dense parcel of gas with $n_H = 1100$ cm^{-3} in a time of 0.3 Myr. At this time the dominant form of carbon in the dense gas is neutral C with the C/CO abundance ratio equal to 30. At significantly longer times, the conversion of C into CO takes place.

Here we report a more ambitious calculation with the extended chemical network of HL in which we follow the continuously varying density of diffuse gas which eventually mixes with a dense parcel. This process is modeled via a three-step process depicted schematically in Figure 4. First, a diffuse parcel of material with the characteristics of parcel 2 ($n_H = 10^2$ cm$^{-3} = n_i$) in Table 1 is allowed to reach steady state, a process which occurs quite rapidly in diffuse regions. Second, the chemistry of this diffuse parcel is followed as it compresses into denser material with the characteristics of parcel 1 ($n_H = 2 \times 10^4$ cm$^{-3} = n_f$) according to the equation

$$n_f = n_i \exp(\omega t_{\rm comp}) \qquad (5)$$

where $t_{\rm comp}$ is the compression time and ω is defined so that the gas compresses to the required density in the time $t_{\rm comp}$. During compression, the visual extinction increases according to the equation

$$A_{v,f}/A_{v,i} = (n_f/n_i)^{2/3} \qquad (6)$$

based on spherically symmetric compression, and the temperature cools according to the relation derived in the Appendix. This second stage is supposed to emulate what happens in realistic mixing as the material increases in density before mixing with the dense parcel. The compressed gas has a low fractional ionization characteristic of one-phase models with low metallic abundances; in other words, the C^+ abundance is now quite small. The chemical effect of compression is not only to produce a large abundance of neutral C out of the initial C^+ but to produce significant abundances of organic molecules. This is depicted in Figures 5*a* and 5*b* which contain plots of the fractional abundances of C and HC_9N respectively as functions of $t/t_{\rm comp}$ for $t_{\rm comp} = 0.2$, 0.5, and 1.0 Myr. The HC_9N abundance is less affected than the C abundance by changes in the compression time because the neutral C is rapidly converting itself into CO.

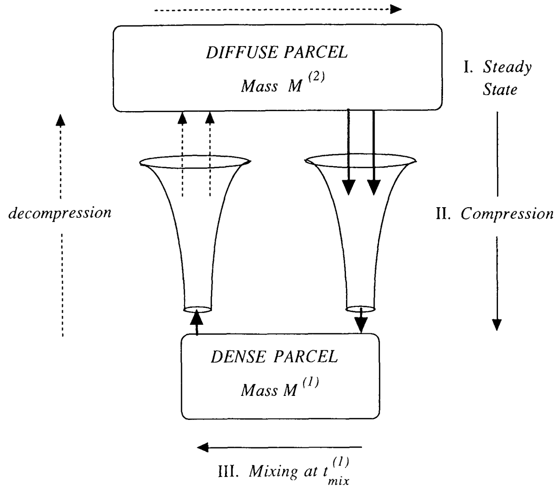

FIG. 4.—A pictorial representation of the approach used to model mixing between diffuse and dense gas in a natural manner. The gas first reaches steady state in stage I and is then compressed in stage II before the mixing actually occurs in stage III. Although not treated in our calculations, recycling into diffuse gas should occur and is shown in the figure. The mass of the diffuse gas $M^{(2)}$ is assumed to be much larger than the mass of the dense gas $M^{(1)}$ so that mixing does not affect the chemical composition of the diffuse gas.

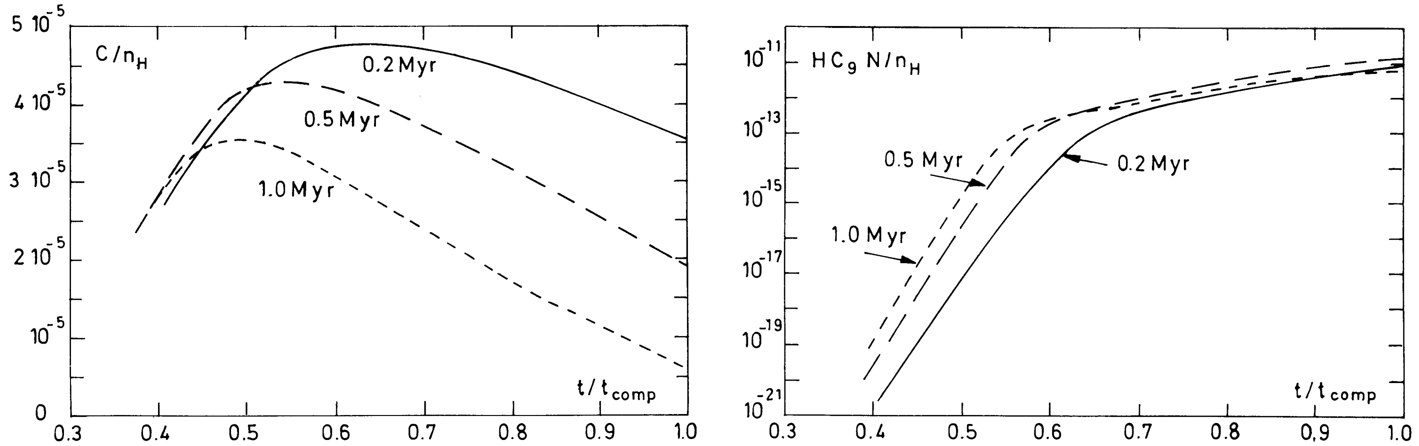

FIG. 5*a*

FIG. 5*b*

FIG. 5.—(*a*) A plot of the fractional abundance of C with respect to n_H vs. time expressed as a fraction of the compression time t_{comp} for three representative compression times. The results are for the compression stage of the three-stage model shown in Fig. 4. (*b*) A plot of the fractional abundance of HC_9N with respect to n_H vs, time expressed as a fraction of the compression time t_{comp} for three representative compression times. The results are for the compression stage of the three-stage model shown in Fig. 4.

In the third stage, the compressed material, now at the same density as the dense parcel of gas *and rich in both C and organic molecules*, mixes with the dense parcel with mixing time $t^{(1)}_{mix}$. The chemistry of the dense parcel is followed to steady state. Organic molecule abundances achieved in the dense parcel reflect both the abundances of the same molecules in the gas with which mixing is occurring and the high abundance of C mixed in. Although the mixing of diffuse gas into dense gas is well represented by this approach, the return of dense gas to diffuse gas is not treated. Despite its pictorial representation in Figure 4, an analogous decompression phase is not considered in this paper because calculations show that decompression merely reverses the chemical effects of compression. Moreover, since the mass fraction of dense clumps is small (roughly a few percent), the mixing time $t^{(2)}_{mix}$ in the low-density parcel, considered as a reservoir, is assumed to be much larger than $t^{(1)}_{mix}$ so that the diffuse gas is not affected by the return material in any event.

In the three-stage model, there are two time parameters: t_{comp} and $t^{(1)}_{mix}$. Physical arguments can be made that each of these should be in the range 0.1–1 Myr. The model is linked to clump formation and evolution in molecular clouds. Whatever the actual mechanism is, one time scale applies to the condensation stage, and a second applies to the lifetime of the gas parcel in its dense phase. In CPF1, it was argued that matter experiences a stretched gravitational collapse. The relevant compression time was directly linked to the mass flux in density space. Note that gravitational collapse leads to compression time scales of the order of 20 $n_H^{-1/2}$ Myr. In another approach, de Boisanger & Chièze (1990) have suggested that fluctuations in the UV radiation field exposure, due to external perturbations in the extinction, trigger the formation and dissolution of dense clumps. The compression time scale is quite short, of the order of a few times 10^5 Myr, and is governed by the nonequilibrium energy balance. The time spent by the gas at high density (i.e., the mixing time) depends only on the linear scale of the perturbation and its velocity and is thus independent of the compression time scale. For example, a clump of size 1 = 0.1 pc, moving with a velocity $v = 0.5$ km s^{-1}, induces a condensation in which the characteristic mixing time is $1/v = 0.2$ Myr.

The steady state fractional abundances for our three-stage model are presented in Table 4 for assorted values of the two time parameters. The salient feature of Table 4 is that there is little dependence of the fractional abundances for both small and large molecules on the two time parameters in the ranges chosen. Changes of at most 1.5 orders of magnitude or so between maximum and minimum values are obtained. In general, the largest abundances of the most complex molecules are achieved at small compression and mixing times, whereas the smallest abundances are achieved at large compression and mixing times. The calculated abundances for all chosen t_{comp} and $t^{(1)}_{mix}$ tend to be quite close to the one-phase early-time values, as can be seen by comparison with the results shown in either Table 2 or 3. If we once again focus on the complex molecule HC_9N, we observe that its steady state fractional abundance with respect to H_2 reaches 4×10^{-11} for the model with $t_{comp} = 0.2$ Myr and $t^{(1)}_{mix} = 0.1$ Myr, which is only a factor of ≈ 2 below the one-phase early-time abundance. Unlike many other molecules, the abundance of HC_9N is calculated to decrease more than an order of magnitude as the time parameters increase to their maximum values. *In general, however, our realistic approach to dynamical mixing can achieve the two goals of removing the time dependence of organic molecule abundances in one-phase models and maintaining large abundances at steady state.*

The (weak) dependence of the assorted results on the two time parameters can be explained as follows. The parameter t_{comp} determines the time necessary for the second stage of the process to be completed. In the exponential compression, the chemistry of organic molecules appears to be rather insensitive to the value of t_{comp} in the range utilized, as can be seen in Figure 5*b*. However, the longer this time, the more complete the conversion of C into CO in the gas being compressed, as can be seen in Figure 5*a*. At much longer t_{comp} the organic molecule abundances in the compressed gas will decrease substantially due to the absence of C, as in one-phase constant density models. At much shorter t_{comp}, there will be insufficient

TABLE 4

SELECTED CALCULATED FRACTIONAL ABUNDANCES[a] AT STEADY STATE VERSUS $t_{\rm comp}$ AND $t_{\rm mix}^{(1)}$ (Myr) FOR THE THREE-STAGE "REALISTIC" MODEL

$t_{\rm comp}$	0.2	0.2	0.2	0.5	0.5	0.5	1.0	1.0	1.0
$t_{\rm mix}^{(1)}$	0.1	0.5	1.0	0.1	0.5	1.0	0.1	0.5	1.0
e	3.9(-08)	3.7(-08)	3.7(-08)	3.7(-08)	3.6(-08)	3.7(-08)	3.7(-08)	3.7(-08)	3.7(-08)
C^+	1.7(-09)	1.2(-09)	1.0(-09)	1.2(-09)	1.0(-09)	8.6(-10)	1.1(-09)	9.2(-10)	8.0(-10)
C	4.2(-05)	1.5(-05)	7.8(-06)	2.2(-05)	7.8(-06)	3.8(-06)	6.8(-06)	2.2(-06)	1.1(-06)
OH	9.6(-08)	1.3(-07)	1.5(-07)	1.2(-07)	1.5(-07)	1.7(-07)	1.4(-07)	1.7(-07)	2.0(-07)
CH	3.0(-08)	1.0(-08)	5.4(-09)	1.4(-08)	5.4(-09)	3.4(-09)	5.0(-09)	3.0(-09)	2.4(-09)
NH	1.1(-10)	4.8(-10)	1.1(-09)	2.0(-10)	7.2(-10)	1.4(-09)	4.8(-10)	1.2(-09)	2.0(-09)
CO	9.4(-05)	1.2(-04)	1.3(-04)	1.1(-04)	1.3(-04)	1.3(-04)	1.3(-04)	1.4(-04)	1.4(-04)
C_2	1.1(-08)	3.8(-09)	2.2(-09)	5.4(-09)	2.6(-09)	1.7(-09)	2.4(-09)	1.6(-09)	1.2(-09)
CN	7.6(-08)	7.0(-08)	5.8(-08)	7.2(-08)	5.8(-08)	4.6(-08)	5.8(-08)	3.8(-08)	2.8(-08)
NO	3.2(-08)	7.6(-08)	1.1(-07)	5.8(-08)	1.2(-07)	1.6(-07)	1.3(-07)	1.9(-07)	2.4(-07)
CH_2	2.2(-07)	1.3(-07)	9.0(-08)	1.6(-07)	8.4(-08)	5.4(-08)	7.6(-08)	3.6(-08)	2.4(-08)
NH_2	1.6(-09)	6.0(-09)	1.3(-08)	2.6(-09)	8.4(-09)	1.6(-08)	5.6(-09)	1.3(-08)	2.2(-08)
H_2O	6.4(-06)	8.2(-06)	7.6(-06)	8.8(-06)	8.4(-06)	7.8(-06)	9.2(-06)	8.0(-06)	6.8(-06)
C_2H	4.4(-08)	1.4(-08)	7.2(-09)	2.0(-08)	7.0(-09)	4.2(-09)	6.2(-09)	3.4(-09)	2.8(-09)
HCN	9.4(-07)	6.8(-07)	3.8(-07)	8.6(-07)	4.8(-07)	2.6(-07)	5.2(-07)	2.4(-07)	1.3(-07)
HNC	3.0(-07)	3.4(-07)	2.0(-07)	3.6(-07)	2.8(-07)	1.6(-07)	3.0(-07)	1.7(-07)	9.6(-08)
NH_3	7.6(-09)	2.6(-08)	5.0(-08)	1.3(-08)	3.4(-08)	5.8(-08)	2.2(-08)	4.8(-08)	7.0(-08)
C_2H_2	6.0(-07)	4.2(-07)	2.8(-07)	6.4(-07)	4.0(-07)	2.8(-07)	4.6(-07)	3.0(-07)	2.0(-07)
H_2CO	8.0(-07)	5.6(-07)	4.0(-07)	8.4(-07)	5.2(-07)	3.6(-07)	5.6(-07)	3.4(-07)	2.4(-07)
C_3H	3.2(-07)	2.2(-07)	1.4(-07)	3.4(-07)	2.2(-07)	1.4(-07)	2.2(-07)	1.3(-07)	9.0(-08)
C_3N	1.2(-09)	7.4(-10)	4.8(-10)	1.0(-09)	6.8(-10)	4.6(-10)	7.8(-10)	5.2(-10)	3.6(-10)
CH_4	4.4(-06)	5.2(-06)	4.6(-06)	6.2(-06)	5.6(-06)	4.4(-06)	6.2(-06)	5.0(-06)	3.8(-06)
C_3H_2	1.5(-07)	1.1(-07)	6.8(-08)	1.5(-07)	1.0(-07)	6.6(-08)	1.1(-07)	6.8(-08)	4.6(-08)
C_4H	2.0(-07)	1.1(-07)	6.4(-08)	1.8(-07)	1.1(-07)	6.6(-08)	9.4(-08)	5.8(-08)	3.6(-08)
HC_3N	1.9(-08)	1.2(-08)	6.4(-09)	2.0(-08)	1.1(-08)	6.0(-09)	1.3(-08)	6.8(-09)	3.8(-09)
C_5H	3.0(-08)	1.8(-08)	9.6(-09)	2.8(-08)	1.7(-08)	1.0(-08)	1.5(-08)	9.6(-09)	5.8(-09)
CH_3OH	4.4(-09)	5.0(-09)	3.0(-09)	7.0(-09)	4.8(-09)	2.8(-09)	5.8(-09)	3.0(-09)	1.7(-09)
C_6H	4.4(-08)	2.2(-08)	1.2(-08)	3.6(-08)	2.0(-08)	1.2(-08)	1.5(-08)	9.0(-09)	5.4(-09)
HC_5N	6.2(-09)	3.6(-09)	1.8(-09)	5.8(-09)	3.6(-09)	1.9(-09)	3.0(-09)	1.8(-09)	1.0(-09)
C_7H	3.0(-09)	1.8(-09)	9.2(-10)	3.0(-09)	1.9(-09)	1.1(-09)	1.5(-09)	9.6(-10)	5.6(-10)
C_8H	5.0(-09)	2.6(-09)	1.4(-09)	4.0(-09)	2.4(-09)	1.3(-09)	1.5(-09)	9.4(-10)	5.6(-10)
CH_3C_3N	3.6(-10)	2.8(-10)	1.3(-10)	5.0(-10)	2.6(-10)	1.2(-10)	3.5(-10)	1.5(-10)	7.0(-11)
HC_7N	3.2(-10)	1.5(-10)	6.0(-11)	2.8(-10)	1.3(-10)	6.2(-11)	1.1(-10)	5.4(-11)	2.6(-11)
CH_3OCH_3	1.4(-12)	2.4(-12)	1.1(-12)	3.6(-12)	2.6(-12)	1.1(-12)	3.2(-12)	1.6(-12)	8.6(-13)
C_9H	3.0(-10)	1.9(-10)	8.8(-11)	3.4(-10)	2.2(-10)	1.1(-10)	1.5(-10)	9.4(-11)	5.2(-11)
HC_9N	4.2(-11)	1.9(-11)	6.8(-12)	3.4(-11)	1.7(-11)	7.4(-12)	1.2(-11)	6.0(-12)	2.6(-12)
H_3^+	1.8(-09)	1.9(-09)	2.0(-09)	1.8(-09)	2.0(-09)	2.2(-09)	2.0(-09)	2.2(-09)	2.2(-09)
HCO^+	4.8(-09)	5.2(-09)	6.0(-09)	4.6(-09)	5.2(-09)	6.0(-09)	5.2(-09)	6.0(-09)	6.8(-09)
N_2H^+	6.6(-12)	5.0(-11)	1.2(-10)	1.5(-11)	7.4(-11)	1.5(-10)	4.6(-11)	1.3(-10)	2.0(-10)
H_3O^+	2.6(-09)	2.6(-09)	2.4(-09)	2.6(-09)	2.4(-09)	2.2(-09)	2.4(-09)	2.2(-09)	2.0(-09)
CH_3^+	7.0(-11)	2.8(-11)	1.5(-11)	3.8(-11)	1.5(-11)	8.6(-12)	1.4(-11)	6.0(-12)	3.6(-12)

NOTE.—*a*(-*b*) refers to $a\ 10^{-b}$.

[a] With respect to H_2.

time to produce complex molecules. The organic molecule abundances in the dense parcel are determined both by their respective abundances in the compressed gas and by the C abundance in the compressed gas, which is a precursor for additional chemical synthesis. Therefore one expects the organic molecule abundances in the dense parcel to decline considerably at much shorter and longer $t_{\rm comp}$ than used here. This expectation has been confirmed by suitable calculations. In the range of $t_{\rm comp}$ depicted in Table 4, the abundances of most complex molecules are slightly larger for the smaller times.

The parameter $t_{\rm mix}^{(1)}$ determines the rate of the mixing of the compressed gas into the dense gas in the third stage of the process. At very short mixing times, the dense gas will simply achieve the abundances of the compressed gas which is rapidly flowing into and out of it. As the mixing rate is slowed, chemical effects in the dense gas will begin to play a role and result in somewhat larger organic molecule abundances by a factor of a few. However, at still longer mixing times, the dense gas will tend toward abundances equal to the steady state values in one-phase models, which are essentially depleted in complex organic molecules. With the range of mixing times in Table 4, the abundances of complex molecules tend to decrease with increasing $t_{\rm mix}^{(1)}$.

Since the calculated results depend to some extent on the two time parameters, it might be possible to account for some of the variation in molecular abundances observed toward various sources by suitable variation of these parameters. Consider, for example, the two dark clouds L134N and TMC-1. Molecular abundances in these regions, which possess similar physical conditions, have been compared by Irvine, Goldsmith, & Hjalmarson (1987). In general, the abundances of organic molecules in L134N are considerably lower than those in TMC-1. In table 5, we compare the ratios of a variety of molecular abundances observed in the two sources with the relevant ratios from two of our three-stage models; the model chosen to represent L134N has $t_{\rm comp} = t_{\rm mix}^{(1)} = 1.0$ Myr whereas the model for TMC-1 has $t_{\rm comp} = 0.2$ Myr and $t_{\rm mix}^{(1)} = 0.1$ Myr. The TMC-1 model normally has the largest abundances of complex molecules while the L134N model has the smallest, mimicking the observational differences.

It can be seen in Table 5 that the theoretical abundance ratios are qualitatively in agreement with the observed values. It does appear, however, that the model results do not show a large enough variation between the two sources for the cyanopolyyne abundance ratios. As regards small molecules, the large ammonia abundance in L134N compared with TMC-1 is reproduced by theory, but the theoretical L134N/TMC-1 abundance ratio calculated for N_2H^+ is far too large. In general, the three-stage approach appears to be a promising method of accounting for observed source-to-source variations in molecular abundances but more work needs to be accomplished in understanding the physical basis behind the time parameters and whether the various values utilized for them are reasonable.

4. CONCLUSIONS

One of the most salient features of pseudo–time-dependent gas phase models of dense interstellar cloud chemistry is the strong time dependence of the abundances of organic molecules. With the standard codes currently in use (e.g., HL), these abundances peak at a time between 1–3 × 10^5 yr after the onset of the chemistry and then decline very sharply. A variety of approaches have been undertaken to delay this sharp decline to perhaps 10^6 yr (Brown & Charnley 1990; Flower & Pineau des Forêts 1990). However, at steady state, calculated abundances of organic molecules are well below those in the well-studied source TMC-1 as well as other nearby dark clouds and a variety of extended regions in the cores of giant molecular clouds not associated with star formation. (The chemistry of star-forming regions is more complex; see Herbst 1990 for a review). The gas phase models all utilize the one-phase approximation despite the obvious clumpy nature of molecular clouds. Dynamical mixing processes between parcels of gas of different densities arise naturally from detailed studies of cloud dynamics (de Boisanger & Chièze 1990), and it is only natural to consider such mixing in chemical models. Utilizing a small chemical network, CPF1 showed that rapid mixing ($t_{\rm mix} \leq 10^6$ yr) from a diffuse envelope into and out of a dense clump can enhance the abundances of C and C^+ in the dense gas at steady state. Because these species are precursors of organic molecules, this result leads to the possibility that large abundances of organic molecules can be maintained at times through steady state. Building on the earlier work of CPF1, we have first constructed simple two-phase chemical models of dense interstellar clouds with the large chemical network of HL.

In the two-phase models reported here, the more diffuse gas is of rather low density and visual extinction so that the dominant form of carbon is C^+. Mixing of this diffuse gas into the denser parcel leads to high abundances of C^+ and a high fractional ionization. The resultant abundances of organic molecules in the dense parcel can show rather complex dependences on time and on mixing time; however, the dominant feature is an enhancement in the steady state abundances which is insufficient to reach the large early-time abundances of one-phase models. The high ionization of the dense parcel appears to be the limiting factor in the enhancements of the steady state organic molecule abundances. It is, however, difficult to determine different physical conditions for the diffuse gas that are much more helpful in maintaining the early-time abundances. The problem is that increased density and/or visual extinction lead eventually to a gas rich in CO, in which C is not dominant. If one artifically reduces the amount of C^+ in the diffuse cloud gas by slowing down the photoionization rate of C, the diffuse gas becomes rich in C rather than C^+ (or CO) and only a large abundance of C is continually transferred into the dense parcel. The result is that the steady state organic molecule abundances approach those achieved at early time in one-phase models. The paucity of C^+ in the gas entering the dense phase can be justified by looking in more detail at the process of mixing—as C^+ mixes from the diffuse into the dense parcel the density increases steadily rather than abruptly. During this path through material of increasing density, the C^+ converts into C long before it converts fully into CO.

In our more realistic model, which incorporates to some extent the idea of a continually varying density between diffuse envelopes and dense clumps, we have considered three stages. In the first stage, the chemistry of a diffuse gas with the physical characteristics shown in Table 1 rapidly attains chemical steady state. The dominant form of carbon in this gas is C^+. In the second stage, the diffuse gas is compressed into a dense, highly extinguished gas at a characteristic time $t_{\rm comp}$. During the compression, the C^+ converts into both C and CO and large abundances of organic molecules are synthesized. In the third stage, the compressed gas mixes with the dense clump. The dense gas is enriched in organic molecules *under steady* *state conditions* via chemical processes utilizing neutral C and via actual mixing of the molecules synthesized during the compression phase. Large abundances of organic molecules are achieved at steady state with a variety of realistic compression and mixing times indicating that the extreme time dependence of one-phase models is alleviated by dynamical mixing. As one can see from the results in Table 4, however, calculated variations in molecular abundances still exist depending on compression and mixing times so that observed abundances in different sources are not predicted to all be the same. For the complex molecule HC_9N in particular, these variations are important. Larger variations can be obtained by choosing different final densities for the second (compression) stage.

Because one-phase pseudo–time-dependent models of dense interstellar clouds represent the chemistry reasonably accurately at early time (HL) and because the steady state results of our C-rich two-phase models and a variety of our three-stage models reproduce the one-phase early-time results, reasonable agreement with observation can be obtained. Given the two additional parameters—t_{comp} and $t_{\mathrm{mix}}^{(1)}$ in our realistic three-stage model, we can also reproduce some of the observed source-to-source variation in molecular abundances by suitable variation of these parameters (see Table 5). However, this is less meaningful in our view than our conclusions that (*a*) the extreme time dependence of organic molecule abundances in one-phase models can be eliminated and (*b*) organic molecule abundances large enough to agree with observation can be maintained at *steady state* in models with dynamical mixing.

The question of adsorption onto the surfaces of dust particles remains to be discussed. Specifically, if one wishes to utilize gas phase models at total times significantly greater than 10^5 yr, there is still the unsolved problem of how to maintain sizeable abundances in the gas phase rather than on the surfaces of dust particles. One possibility involves photodesorption during the diffuse stages of the cycle shown in Figure 4, as originally suggested by Boland & De Jong (1982). Another possibility involves shock waves (Williams 1988).

The three-stage model considered here is only an attempt at a grand synthesis of the chemistry and physical evolution of interstellar clouds. Many improvements can be envisaged and will be the subject of future work. Turbulence and clump formation imply strongly that condensation and mixing are at work in molecular clouds. A next step should be to put tighter constraints on dynamical time scales from the observed chemical abundances in molecular clouds. The present trend favors time scales of 0.1–1.0 Myr.

TABLE 5

COMPARISON OF THREE-STAGE MODEL RESULTS WITH ABUNDANCE RATIOS BETWEEN L134N AND TMC-1

Species	L134N/TMC-1[a]	Theory[b]
CO	1.0	1.5
OH	0.25	2.1
CH	0.5	0.1
CCH	<1.0	0.1
C_4H	0.05	0.2
C_3H_2	<0.2	0.3
CH_3CCH	<0.2	2.7
CN	<0.1	0.4
HCN	0.2	0.1
HNC	0.3	0.3
CH_3CN	<1.0	0.1
HC_3N	0.03	0.2
HC_5N	0.03	0.2
C_3N	<0.2	0.3
N_2H^+	1.0	30.0
NH_3	10.0	9.2
HCO^+	1.0	1.4
CH_3OH	1.0	0.4
H_2CO	1.0	0.3

[a] Taken from Irvine et al. 1987. The order of species is such that hydrocarbons precede nitrogen-containing molecules which in turn precede oxygen-containing species.

[b] The model results for L134N have time parameters $t_{\mathrm{comp}} = t_{\mathrm{mix}}^{(1)} = 1.0$ Myr while those for TMC-1 have $t_{\mathrm{comp}} = 0.2$ Myr and $t_{\mathrm{mix}}^{(1)} = 0.1$ Myr.

E. H. wishes to acknowledge the support of the National Science Foundation for his research program in astrochemistry. He is also grateful to the CEA (France) and J. P. Chièze in particular for supporting his stay at Bruyères-le-Châtel while this paper was being written.

APPENDIX

1. MIXING EQUATIONS

Consider two parcels of gas with constant masses $M^{(1)}$ and $M^{(2)}$ and constant mass densities $\rho^{(1)}$ and $\rho^{(2)}$. Also consider a species x with masses $M_x^{(1)}$ and $M_x^{(2)}$ and mass fractions $X^{(1)}$ and $X^{(2)}$ in the two parcels of gas. The time rate of change of $M_x^{(1)}$ due to mixing is given by the equation

$$dM_x^{(1)}/dt = -X^{(1)}dM^{1\rightarrow 2}/dt + X^{(2)}dM^{2\rightarrow 1}/dt\,, \tag{A1}$$

where the time derivatives of the masses of the parcels are set equal because constant overall masses are to be maintained. If we label these derivatives by dM/dt and note that

$$M_x^{(1)} = X^{(1)}M^{(1)}\,, \tag{A2}$$

we obtain from equation (A1) that

$$dX^{(1)}/dt = -X^{(1)}/M^{(1)}dM/dt + X^{(2)}/M^{(1)}dM/dt\,. \tag{A3}$$

Because the mass fraction $X^{(1)}$ can be written as

$$X^{(1)} = n_x^{(1)}m_x/\rho^{(1)}\,, \tag{A4}$$

where $n_x^{(1)}$ is the number density of species x in parcel 1, m_x is the atomic mass of x, and a similar equation holds for $X^{(2)}$, equation (A3) can be rewritten as

$$dn_x^{(1)}/dt = -(n_x^{(1)} - n_x^{(2)}\rho^{(1)}/\rho^{(2)})(M^{(1)})^{-1}dM/dt \tag{A5}$$

after cancellation of m_x. Equation (A5) yields the change in concentration of species x in parcel 1 due to mixing.

2. TIME DEPENDENCE OF TEMPERATURE

In this derivation, the superscripts labelling the parcels are omitted for clarification. The specific energy ϵ per unit mass of a gas parcel is given in terms of the temperature T by the equation

$$\epsilon = 3kT/2\mu\ , \tag{A6}$$

where μ is the average mass of a species in the parcel and k is the Boltzmann constant. Only translational energy is included. The time rate of change of ϵ is given by the equation

$$d\epsilon/dt = B/\rho + P/\rho^2 d\rho/dt\ , \tag{A7}$$

where B is the net heating rate per unit volume, P is the pressure, and ρ is the mass density, which is assumed to be constant in the simple two-phase model. The mass density in turn can be related to μ by the relation.

$$\rho = \mu n\ , \tag{A8}$$

in which n is the overall number density. Then

$$1/\rho\, d\rho/dt = 1/\mu\, d\mu/dt + 1/n(dn/dt)_{\rm chem} + 1/n(dn/dt)_{\rm mech}\ , \tag{A9}$$

where the variations of n due to chemistry and mechanical compression are treated separately. Since the last term on the right-hand side of (A9) equals the left-hand side, it follows that

$$d\mu/dt = -(\mu/n)(dn/dt)_{\rm chem}\ . \tag{A10}$$

Inversion of equation (A6) and taking the time derivative of T leads to

$$dT/dt = 2\mu B/3k\rho + 2/3 T/\rho\, d\rho/dt + (2\epsilon/3k)\, d\mu/dt\ , \tag{A11}$$

via substitution of equation (A7) and the ideal gas law. Finally, substitution of equations (A6), (A8), and (A10) and the ideal gas law lead to the result that

$$1/T\, dT/dt = 2B/3P - 1/n\,(dn/dt)_{\rm chem} + 2/3\ 1/\rho\, d\rho/dt\ . \tag{A12}$$

REFERENCES

Black, J. H. 1987, in Interstellar Processes, ed. D. J. Hollenbach & H. A. Thronson, Jr. (Dordrecht: Reidel), p. 731

Boland. W., & De Jong, T. 1982, ApJ, 261, 110

———. 1984, A&A, 134, 87

Brown, P. D., & Charnley, S. B. 1990, MNRAS, 244, 432

Charnley, S. B., Dyson, J. E., Hartquist, T. W., & Williams, D. A. 1988a, MNRAS, 231, 269

———. 1988b, MNRAS, 235, 1257

Chièze, J. P., & Pineau des Forêts, G. 1987, A&A, 183, 98

———. 1989, A&A, 221, 89 (CPF1)

———. 1990, in Physical Processes in Fragmentation and Star Formation, ed. R. Capuzzo-Dolcetta, C. Chiosi, & A. Di Fazio (Dordrecht: Kluwer), p. 17 (CPF2)

de Boisanger, C., & Chièze, J. P. 1990, A&A, in press

Flower, D. R., & Pineau des Forêts, G. 1990, MNRAS, 247, 500

Flower, D. R., Pineau des Forêts, G., & Hartquist, T. W. 1986, MNRAS, 218, 729

Genzel, R., Harris, A. I., Jaffe, D. T., & Stutzki, J. 1988, ApJ, 332, 1049

Graedel, T. E., Langer, W. D., & Frerking, M. A. 1982, ApJS, 48, 321

Gredel, R., Lepp, S., & Dalgarno, A. 1987, ApJ, 323, L137

Gredel, R., Lepp, S., Dalgarno, A., & Herbst, E. 1989, ApJ, 347, 289

Herbst, E. 1990, in Physical Processes in Fragmentation and Star Formation, ed. R. Capuzzo-Dolcetta, C. Chiosi, & A. Di Fazio (Dordrecht: Kluwer), p. 3

Herbst, E., & Klemperer, W. 1973, ApJ, 185, 505

Herbst, E., & Leung, C. M. 1989, ApJS, 69, 271 (HL)

———. 1990, A&A, 233, 177

Herbst, E., & Millar, T. J. 1991, in Molecular Clouds, ed. R. J. James & T. J. Millar (London: Cambridge University Press), in press

Irvine, W. M., Goldsmith, P. F., & Hjalmarson, Å, 1987, in Interstellar Processes, ed. D. J. Hollenbach & H. A. Thronson, Jr. (Dordrecht: Reidel), p. 561

Keene, J., Blake, G. A., Phillips, T. G., Huggins, P. J., & Beichman, C. A. 1985, ApJ, 299, 967

Langer, W. D., & Graedel, T. E. 1989, ApJS, 69, 241

Langer, W. D., Graedel, T. E., Frerking, M. A., & Armentrout, P. B. 1984, ApJ, 277, 581

Leung, C. M., Herbst, E., and Huebner, W. F. 1984, ApJS, 56, 231

Millar, T. J., & Herbst, E. 1990, A&A, 231, 466

Millar, T. J., Leung, C. M., & Herbst, E. 1987, A&A, 183, 109

Millar, T. J., & Nejad, L. A. M. 1985, MNRAS, 217, 507

Phillips, T. G., & Huggins, P. J. 1981, ApJ, 251, 533

Prasad, S. S., & Huntress, W. T., Jr. 1980a, ApJS, 43, 1

———. 1980b, ApJ, 239, 151

Prasad, S. S., & Tarafdar, S. P. 1983, ApJ, 267, 603

Scalo, J. 1990, in Physical Processes in Fragmentation and Star Formation, ed. R. Capuzzo-Dolcetta, C. Chiosi, & A. Di Fazio (Dordrecht: Kluwer), p. 151

Smith, I. M. W. 1989, ApJ, 347, 282

Stutzki, J., Stacey, G. J., Genzel, R., Harris, A. I., Jaffe, D. T., & Lugten, J. B. 1988, ApJ, 332, 379

Talbi, D., & DeFrees, D. J. 1990, Chem. Phys. Letters, submitted

Tarafdar, S. P., Prasad, S. S., Huntress, W. T., Jr., Villere, K. R., & Black, D. C. 1985, ApJ, 289, 220

Tielens, A. G. G. M., & Hollenbach, D. 1985a, ApJ, 291, 722

———. 1985b, ApJ, 291, 747

van Dishoeck, E. F., & Black, J. H. 1988, ApJ, 334, 771

Williams, D. A. 1988, in Rate Coefficients in Astrochemistry, ed. T. J. Millar & D. A. Williams (Dordrecht: Kluwer), p. 281

Winnewisser, G., & Herbst, E. 1987, Topics Current Chem., 139, 119